Molecular Biology of the Cell
Vol. 10, 2687–2702, August 1999

Clathrin Assembly Lymphoid Myeloid Leukemia (CALM) Protein: Localization in Endocytic-coated Pits, Interactions with Clathrin, and the Impact of Overexpression on Clathrin-mediated Traffic

Francesc Tebar,* Stefan K. Bohlander,† and Alexander Sorkin*‡

*Department of Pharmacology, University of Colorado Health Science Center, Denver, Colorado 80111; and †Institute of Human Genetics, 37073 Goettingen, Germany

Submitted December 16, 1998; Accepted May 18, 1999
Monitoring Editor: Juan Bonifacino

The clathrin assembly lymphoid myeloid leukemia (*CALM*) gene encodes a putative homologue of the clathrin assembly synaptic protein AP180. Hence the biochemical properties, the subcellular localization, and the role in endocytosis of a CALM protein were studied. In vitro binding and coimmunoprecipitation demonstrated that the clathrin heavy chain is the major binding partner of CALM. The bulk of cellular CALM was associated with the membrane fractions of the cell and localized to clathrin-coated areas of the plasma membrane. In the membrane fraction, CALM was present at near stoichiometric amounts relative to clathrin. To perform structure–function analysis of CALM, we engineered chimeric fusion proteins of CALM and its fragments with the green fluorescent protein (GFP). GFP–CALM was targeted to the plasma membrane–coated pits and also found colocalized with clathrin in the Golgi area. High levels of expression of GFP–CALM or its fragments with clathrin-binding activity inhibited the endocytosis of transferrin and epidermal growth factor receptors and altered the steady-state distribution of the mannose-6-phosphate receptor in the cell. In addition, GFP–CALM overexpression caused the loss of clathrin accumulation in the trans-Golgi network area, whereas the localization of the clathrin adaptor protein complex 1 in the trans-Golgi network remained unaffected. The ability of the GFP-tagged fragments of CALM to affect clathrin-mediated processes correlated with the targeting of the fragments to clathrin-coated areas and their clathrin-binding capacities. Clathrin–CALM interaction seems to be regulated by multiple contact interfaces. The C-terminal part of CALM binds clathrin heavy chain, although the full-length protein exhibited maximal ability for interaction. Altogether, the data suggest that CALM is an important component of coated pit internalization machinery, possibly involved in the regulation of clathrin recruitment to the membrane and/or the formation of the coated pit.

INTRODUCTION

Clathrin-mediated vesicle formation is an essential step in endocytosis and the intracellular trafficking of macromolecules. Clathrin-coated pits located at the plasma membrane and the trans-Golgi network (TGN) serve to form transport vesicles destined to various endosomal compartments (reviewed in Schmid, 1997; Traub and Kornfeld, 1997). Clathrin coats are also found on endosomes (Stoorvogel *et al.*, 1996). However, the role of these coats is not defined. The major structural components of clathrin-coated pits are the clathrin triskelions and the clathrin adaptor protein complexes or APs. Each AP is a heterotetramer consisting of two large, one medium, and one small subunit (reviewed in Robinson, 1997). AP-2 functions at the plasma membrane, and AP-1 functions at the TGN. Another tetrameric protein complex, AP-3, is found in endosomes in mammalian cells (reviewed in Odorizzi *et al.*, 1998); however the function of AP-3 and whether it participates in clathrin coats are under debate.

Besides structural elements of the coat, a growing number of proteins associated with clathrin-coated pits and vesicles

‡ Corresponding author. E-mail address: alexander. sorkin@uchsc.edu.

Abbreviations used: AMCA, 7-amino-4-methylcoumarin-3-acetic acid; AP, clathrin adaptor protein complex; CALM, clathrin assembly lymphoid myeloid leukemia; CHC, clathrin heavy chain; CMF-PBS, Ca^{2+}- and Mg^{2+}-free phosphate-buffered saline; EGF, epidermal growth factor; EH, Eps15 homology; GFP, green fluorescent protein; GST, glutathione-*S*-transferase; IgG, immunoglobulin G; M6P, mannose-6-phosphate; TD, terminal domain of CHC; TGN, trans-Golgi network; TRF–TR, transferrin conjugated with Texas Red; TX100, Triton X-100.

are being identified. These proteins participate in multiple protein–protein interactions and enzymatic activities that control the dynamic cycle of coat assembly and disassembly. This cycle begins with the attachment of APs and, subsequently, clathrin triskelions to the membrane leading to the formation of a polyhedral lattice, continues during recruitment of cargo proteins, coat invagination, and vesicle scission, and ends with the release of the coat elements from the vesicle to the cytosol followed by their recycling back to the donor membrane.

One of the major components of brain clathrin-coated vesicles is AP180 (also known as AP-3, NP185, pp155, Fl-20) (Ahle and Ungewickell, 1986; Keen and Black, 1986; Kohtz and Puszkin, 1988; Lindner and Ungewickell, 1992; Zhou *et al.*, 1992). AP180 is located in clathrin-coated buds in the nerve terminal plasma membrane (Takei *et al.*, 1996). AP180 is capable of binding to clathrin triskelions and cages and of promoting the assembly of clathrin coats in vitro (Lindner and Ungewickell, 1992; Ye and Lafer, 1995a,b). Both N- and C-terminal regions of AP180 have the ability to bind clathrin triskelions, although only the C-terminal part promotes coat assembly and binds to clathrin cages (Ye and Lafer, 1995a,b). AP180 also binds phosphoinosides and inositolphosphates via its N-terminal domain (Norris *et al.*, 1995; Ye *et al.*, 1995; Hao *et al.*, 1997). Despite extensive biochemical characterization of AP180, almost no information is available regarding the function of AP180 in vivo.

Yeast homologues of AP180 have been identified, and their binding to clathrin has been demonstrated (Wendland and Emr, 1998). The deletion of yeast AP180 genes had no significant effect on endocytosis (Wendland and Emr, 1998). Recently, the *Drosophila* homologue of AP180 (LAP) has been cloned (Zhang *et al.*, 1998). A mutation that eliminates LAP severely impairs synaptic vesicle endocytosis and alters the normal localization of clathrin in nerve terminals. Most importantly, the size of synaptic vesicles is significantly increased in *lap* mutants.

Recently a human gene that displayed substantial sequence similarity to rat AP180 was found to be involved in the t(10;11) chromosomal translocation, a rare translocation found in lymphoid as well as in myeloid acute leukemias, and was named *CALM* for the clathrin assembly lymphoid myeloid leukemia gene (Dreyling *et al.*, 1996). *CALM* transcripts were detected in all tissues tested, and therefore it was proposed that CALM is a nonneuronal homologue of AP180. The properties of the CALM protein have not been characterized.

In this study the molecular interactions and subcellular localization of the CALM protein were investigated. The data demonstrate that clathrin is the major binding partner of CALM. Overexpression of clathrin-binding fragments of CALM dramatically affects clathrin-mediated endocytosis and the trafficking of receptors between the TGN and endosomes. The data suggest an important role for CALM in the regulation of clathrin internalization machinery.

MATERIALS AND METHODS

Reagents

Iron-saturated transferrin conjugated with Texas Red (TRF–TR) was purchased from Molecular Probes (Eugene, OR). Human recombinant epidermal growth factor (EGF) was obtained from Collaborative Research (Bedford, MA). Mouse receptor-grade EGF was iodinated using a modified chloramine T method as described previously (Carpenter and Cohen, 1976). The specific activity of ^{125}I-labeled EGF was 1.5–1.9 $\times$ 10^5 cpm/ng. A polyclonal antibody to the cation-independent mannose-6-phosphate (M6P) receptor is a gift of Dr. L. Macovcik (Yale University, New Haven, CT). Monoclonal antibodies to the clathrin heavy chain (X.22 and TD.1) and the α-subunits of AP-2 (AP.6) (Brodsky, 1985) were obtained from American Type Culture Collection (Rockville, MD), whereas the monoclonal 100/3 specific to γ-adaptin was from Sigma (St. Louis, MO). AC1-M11 antibody was purchased from Affinity Bioreagents (Golden, CO). Polyclonal antibodies were either used as the immunoglobulin G (IgG) fraction purified from serum using Protein A-Sepharose (Sigma) or affinity-purified. Rabbit antibody to CALM was raised to the purified N-terminal fragment of CALM (residues 1–413) obtained by proteolytic digestion of the glutathione-*S*-transferase (GST)–1–413 fragment of CALM and affinity-purified using this fragment covalently immobilized on CNBr-Sepharose.

Cloning of the CALM Expression Constructs

DNA encoding CALM full-length cDNA and its fragments corresponding to residues 1–413 and 414–652 were obtained by PCR using CALM cDNA (Dreyling *et al.*, 1996). Primers were designed to express CALM as N-terminal fusion proteins with GST in the pGEX-5X-1 vector (Pharmacia, Piscataway, NJ) using *Bam*HI and *Not*I restriction sites.

A bright green fluorescence mutant of green fluorescent protein (GFP), enhanced GFP (Clontech, Palo Alto, CA), was attached to the N or C terminus of full-length CALM or its fragments by standard recombinant PCR techniques. Primers containing *Bgl*II (forward) or *Kpn*I (backward) restriction sites were designed to clone full-length CALM (amino acid residues 1–652) and N-terminal (residues 1–413, 1–304) or C-terminal (residues 414–652) fragments. These were cloned into the pEGFP-C1 to produce GFP–CALM, GFP–1–413, GFP–1–304, and GFP–414–652, respectively, and into pEGFP-N1 to produce CALM–GFP, 1–414–GFP, and 1–303–GFP. Backward primers containing a stop codon were designed to clone full-length CALM and fragments 1–413 and 1–304 into pEGFP-N1 to obtain constructs encoding untagged proteins. To clone GFP–1–613 and GFP–414–613 fusion proteins, we digested GFP–CALM and GFP–414–652 with *Bgl*II and *Eco*RI (internal site), and the liberated fragments 1–613 and 414–613 were cloned into *Bgl*II/*Eco*RI sites of pEGFP-C1. To create GFP–613–652, we digested GFP–CALM with *Bgl*II and *Eco*RI (internal site) to remove fragment 1–612, and the sticky ends were blunted by end filling and ligated together.

Metabolic Cell Labeling and Protein–Protein Interactions

HeLa cells were incubated with ^{35}S-TransLabel (ICN Biochemicals, Costa Mesa, CA) overnight in methionine-free media and 1% dialyzed serum. The cells were washed with Ca^{2+}- and Mg^{2+}-free phosphate-buffered saline (CMF-PBS) and then permeabilized using buffer A (150 mM KCl, 2 mM $MgCl_2$, 20 mM HEPES, 10% glycerol, pH 7.2, 1 mM dithiothreitol, 1 mM EGTA, 1 mM EDTA, 1 mM sodium orthovanadate, 10 mM sodium fluoride, 1 mM phenylmethylsulfonyl fluoride, 10 μg/ml leupeptin, 544 μM iodoacetamide, 10 μg/ml aprotinin) supplemented with 0.02% saponin by scraping from the dish with a rubber policeman and incubated for 15 min at 4°C to allow the release of the cytosolic proteins. The saponin (cytosolic) fraction was then centrifuged at 14,000 $\times$ *g* for 10 min. The membrane fractions were solubilized with buffer A supplemented with 1% Triton X-100 (TX100) and 1% sodium deoxycholate.

GST–CALM, GST–1–413, or GST–414–652 immobilized on glutathione-agarose beads was incubated with the cytosol or membrane fractions of the [^{35}S]methionine-labeled cells for 3 h at 4°C. After extensive washes of the beads with buffer A, the beads were heated at 90°C for 5 min in sample buffer, the bound proteins were

resolved on 7.5% SDS-PAGE, and proteins were transferred to nitrocellulose membranes and analyzed by autoradiography and Western blotting (Sorkin *et al.*, 1996).

Cell Culture and Transfections

HeLa cells were grown in DMEM containing 10% fetal bovine serum, gentamycin, and glutamine. COS-1 cells were grown in DMEM containing 10% newborn calf serum, antibiotics, and glutamine. Cells grown to 50–80% confluency were transfected with pEGFP-CALM DNAs using lipofectamine (Life Technologies, Gaithersburg, MD) or Effectene (Qiagen, Hilden, Germany). Transient transfections were used for all experiments with COS-1 and HeLa cells. The number of transfected cells, estimated by GFP fluorescence, varied from 30 to 70% in different experiments. Transfected cells were split 1 d after transfection to dishes and glass coverslips and used for experiments on the second or third day. Cells were grown to ~90 or 50% confluency for coimmunoprecipitation or immunofluorescence experiments, respectively.

Immunoprecipitation and Western Blotting

Cells grown on 35-mm dishes were washed with CMF-PBS and solubilized by scraping with a rubber policeman in buffer A containing 1% TX100 and by incubating further for 10 min at 4°C. Lysates were then centrifuged at 14,000 × *g* for 10 min. Supernatants were incubated with rabbit Ab20 specific to CALM, rabbit anti-GFP (Clontech), or monoclonal antibody X.22 to clathrin heavy chain (CHC) for 3–15 h at 4°C and then 30–60 min after the addition of Protein A-Sepharose (Sigma) or Protein G-Sepharose (Zymed, San Francisco, CA), respectively. Normal rabbit or mouse IgG (Zymed) were used as a nonspecific control.

Immunoprecipitates were washed twice with buffer A containing TX100 supplemented with 100 mM NaCl and then once without NaCl. Proteins were separated on 7.5% SDS-PAGE, transferred to nitrocellulose membranes, and immunoblotted as described above. The nitrocellulose membranes were probed with Ab20, TD.1 specific to CHC, and monoclonal or polyclonal anti-GFP. To detect primary mouse or rabbit antibodies, sheep anti-mouse IgG (Cappel, West Chester, PA) or Protein A (Zymed) conjugated with horseradish peroxidase were used, respectively. Enhanced chemiluminescence (Pierce Chemical, Rockford, IL) was used for detection of the horseradish peroxidase reaction.

Cell Fractionation

Cells were mildly permeabilized by scraping from the dish with a rubber policeman in buffer A containing 0.02% saponin and incubated for 15 min at 4°C to allow the release of the cytosolic proteins. The saponin (cytosolic) fraction was then centrifuged at 14,000 × *g* for 10 min. This centrifugation was sufficient to pellet the saponin-permeabilized cells without the loss of membranes, demonstrated by the lack of detectable receptors for EGF in the supernatant. The high-speed centrifugation of saponin-permeabilized cells at 100,000 × *g* for 20 min instead of 14,000 × *g* did not change the distribution of CALM and clathrin between cellular fractions.

The pellet of saponin-permeabilized cells was broken by pipetting in buffer A containing 1% TX100 and incubated further for 10 min at 4°C. The TX100 lysates were centrifuged at 14,000 × *g* for 10 min to obtain a TX100-soluble fraction, and the pellets were solubilized in preheated SDS sample buffer followed by sonication to obtain a TX100-insoluble fraction. Several different aliquots of the saponin and TX100-soluble and -insoluble fractions were processed for electrophoresis and Western blot analysis to detect CHC (antibody TD.1), CALM (Ab20), α-adaptins (antibody AC1-M11), and γ-adaptin (antibody 100/3).

As the protein standard in Western blot detection of CHC, the GST-fused N-terminal fragment of CHC corresponding to residues 1–579 (GST–TD, the fragment recognized by TD.1) was used. The plasmid was kindly provided by Dr. J. Keen (Thomas Jefferson University, Philadelphia, PA). In each experiment, various amounts of GST–TD and the fragment 1–413 of CALM (recognized by Ab20) obtained by removing the GST moiety from GST–1–413 were processed by SDS-PAGE and Western blotting. The concentrations of the recombinant proteins were determined by measuring the UV absorbance at 280 nm and using the molar extinction coefficient ϵ_M values at 280 nm of 18,670 $M^{-1}cm^{-1}$ and 89,110 $M^{-1}cm^{-1}$ for CALM fragment 1–413 and GST–TD, respectively, which were calculated according to Gill and von Hippel (1989). All stages of the Western blotting and the chemiluminescence detection of the recombinant protein standards and cellular fractions were performed simultaneously in the same solutions. The amount of protein was quantitated using densitometry of several films obtained after various lengths of exposure times with the same blot and analyzed using a Molecular Analyst software (Bio-Rad, Richmond, CA). The calibration curves were built in each experiment, and the concentrations of the proteins in cellular fractions were determined by interpolation from the calibration curves within the linear range of immunoblotting detection. The molar amounts of CHC and CALM in the cellular fractions were then calculated.

Endocytosis of Transferrin

Transfected cells grown on coverslips were incubated for 30 min in binding medium (DMEM, 0.1% bovine serum albumin) to deplete the transferrin present in serum and then incubated with 5 μg/ml TRF–TR for 10–15 min at 37°C. Cells were then washed with CMF-PBS and fixed with paraformaldehyde. The fixed cells were either mounted for microscopy or permeabilized and processed for immunofluorescence staining as described below.

The effect of CALM expression on TRF–TR endocytosis was quantitated by analyzing several hundred cells in each preparation. The number of cells with or without significant accumulation of TRF–TR was scored in two groups of the cells: 1) cells that express a high amount of a GFP fusion protein but preserve normal cell morphology and 2) cells that express a low or moderate amount of or no GFP fusion proteins. The effect on endocytosis was expressed as the percent of cells without TRF–TR of the total number of cells of each group.

Immunofluorescence Staining

For staining with Ab20, cells grown on coverslips were washed with CMF-PBS and fixed in methanol at −20°C for 5 min. In experiments in which costaining of Ab20 and AP.6 or 100/3 was performed, the methanol fixation was followed by the incubation of fixed cells with acetone for 5 min at −20°C. To examine the localization of proteins in TX100-treated cells, we incubated cells grown on coverslips with 0.02% saponin in buffer A for 15 min at 4°C and then with 1% TX100 in buffer A for 10 min at 4°C. After the rinse with CMF-PBS, the permeabilized cells were fixed with methanol/acetone. Cells expressing GFP fusion proteins were fixed with freshly prepared 4% paraformaldehyde (Electron Microscopy Sciences, Fort Washington, PA) for 12 min at room temperature and mildly permeabilized using a 3-min incubation in CMF-PBS containing 0.1% TX100 and 0.1% BSA at room temperature.

Coverslips with cells fixed with methanol or formaldehyde were then incubated in CMF-PBS containing 1% BSA at room temperature for 1 h with the primary antibody, washed intensively, and then incubated with the secondary donkey anti-mouse IgG labeled with Texas Red (Jackson ImmunoResearch, West Grove, PA). Both primary and secondary antibody solutions were precleared by centrifugation at 100,000 × *g* for 10 min. For triple-label fluorescence experiments, TRF–TR and GFP fluorescence was visualized simultaneously with anti-clathrin X.22 detected with the secondary antibody labeled with 7-amino-4-methylcoumarin-3-acetic acid (AMCA; emission at 450 nm; Jackson ImmunoResearch). After staining, the coverslips were mounted in Fluoromount-G (Fisher

Scientific, Pittsburgh, PA) containing 1 mg/ml para-phenylenediamine.

The samples were analyzed using digital deconvolution microscopy. A Nikon (Garden City, NY) Diaphot 300 microscope equipped with a 100 × 1.4 numerical aperture oil immersion objective lens and the single fluorochrome filter sets for either Texas Red, fluorescein, or AMCA/DAPI (Chroma, Brattleboro, VT) were used for visualization and recording of the images. To obtain high-resolution three-dimensional images of cells, an imaging workstation consisting of the thermoelectrically cooled charged-coupled device Micromax camera with the Sony Interline area array (Princeton Instruments, Trenton, NJ), the Nikon Diaphot microscope equipped with a z-step motor, and the dual filter wheel controlled by QED Imaging or Intelligent Imaging Innovation (3I, Denver, CO) software was used. Typically, 15–40 serial two-dimensional images were recorded at 100- to 200-nm intervals. A Z-stack of images obtained was deconvoluted using a modification of the constrained iteration method on a DeltaVision workstation (Applied Precision, Issaquah, WA) or using 3I software. The final arrangement of images was performed using Adobe Photoshop 4.03.

Living Cell Fluorescence Imaging of GFP

COS-1 cells transiently expressing GFP fusion proteins were grown in glass chambers (Bioptechs, Butler, PA). The chamber was mounted onto the microscope stage, and the image acquisition through the narrow GFP (excitation 492/10 nm) channel was started. Typically, 50–100 images were acquired every 1–2 s (0.3 s exposure) at room temperature using the QED Imaging workstation as described for immunofluorescence experiments. Binning 2 × 2 or "no binning" modes were used.

Internalization of ^{125}I-labeled EGF

To monitor ^{125}I-labeled EGF internalization, COS-1 cells grown in 12-well dishes were incubated with ^{125}I-labeled EGF in binding medium at 37°C for 1–10 min. The concentration of ^{125}I-labeled EGF was 2 ng/ml to avoid saturation of the internalization machinery. After the indicated times, the medium was aspirated, and the monolayers were rapidly washed three times with DMEM to remove unbound ligand. The cells were then incubated for 5 min with 0.2 M acetic acid, pH 2.8, containing 0.5 M NaCl at 4°C. The acid wash was combined with another short rinse in the same buffer and used to determine the amount of surface-bound ^{125}I-labeled EGF. Finally the cells were lysed in 1 M NaOH to determine the internalized radioactivity. The ratio of internalized to surface radioactivity was plotted against time. The linear regression coefficient of the dependence of this ratio for time represents the specific rate constant for internalization. Nonspecific binding was measured for each time point in the presence of a 100-fold molar excess of unlabeled EGF and was not >3–5% of the total counts.

RESULTS

Identification of CALM Protein and Its Interaction with Clathrin

To identify the product of the *CALM* gene, we purified the GST fusion protein of the N-terminal fragment of CALM (1–413), cleaved the GST moiety, and used the fragment to raise a polyclonal antibody, Ab20. The recognition site of the antibody is between residues 304 and 413 because Ab20 did not recognize the fragment corresponding to residues 1–303. Western analysis with affinity-purified Ab20 detected two specific bands of 72 and 66 kDa in lysates of human HeLa and monkey COS-1 cells (Figure 1A). The size of the larger band agrees well with the predicted molecular mass of full-length CALM of 71.5 kDa. The recombinant CALM transiently expressed in COS-1 cells has the same mobility on SDS-PAGE as the slow-migrating form of endogenous CALM (Figure 1A). Both forms of endogenous CALM could be detected in the immunoprecipitates of Ab20 (Figure 1B). The specificity of Ab20 was also confirmed by immunoprecipitation of recombinant CALM cloned as a fusion protein with the GFP and transiently expressed in HeLa cells (Figure 1C). In the Western blotting assay, Ab20 specifically recognized GFP–CALM precipitated with anti-GFP (Figure 1C).

CALM was detected in all cell lines tested as well as in bovine brain lysates and coated vesicles isolated from bovine brain. Whereas more of the larger form of CALM was expressed in HeLa cells, the smaller form was predominant in COS-1 (Figure 1A), NIH 3T3, and several other cell types (our unpublished data). It is possible that the smaller form is a proteolytic product or an alternative-splicing variant. The differential expression supports the latter possibility. In fact, two alternatively spliced forms of human CALM with an internal deletion of 7 or 50 amino acid residues were reported previously (Dreyling *et al.*, 1996) (Figure 2). The "short" form of human CALM (lacking 49 residues) may correspond to a 66-kDa species of CALM detected by Ab20.

Western blot analysis shows that CALM does not display an abnormally slow mobility on SDS-PAGE that is observed for AP180 (Murphy *et al.*, 1991). The sequence comparison of human CALM and AP180 molecules reveals that CALM displays significant sequence identity to AP180 in the N-terminal part of the molecule (1–300) and in several stretches of the C-terminal domain (Figure 2). The slow mobility of AP180 is presumably caused by the acidic region between residues 305 and 360 (Murphy *et al.*, 1991) that is absent in CALM.

On the basis of the sequence similarity of CALM and AP180, it can be anticipated that CALM would bind clathrin and localize to clathrin-coated pits. As expected, a substantial amount of CHC immunoreactivity was detected in CALM immunoprecipitates from TX100 lysates of HeLa cells (Figure 1B). The immunoprecipitation of GFP–CALM expressed in HeLa cells by anti-GFP also brings down CHC (Figure 1C).

Immunofluorescence staining of HeLa cells with Ab20 required methanol fixation and revealed a punctate pattern of staining typical of clathrin-coated pits (Figure 3). There was also nonspecific staining of cell nuclei as commonly seen in methanol-fixed cells labeled with any rabbit IgG. Double-label immunofluorescence and digital deconvolution of three-dimensional images reveal significant colocalization of CALM and clathrin immunoreactivities, although some dots were stained only with antibodies to clathrin or CALM (Figure 3, A–C). There are two major sites of clathrin localization in the cell: coated buds at the plasma membrane and in TGN containing AP-2 and AP-1, respectively. Therefore, we tested which subset of coats contains CALM. Figure 3, D–F, shows almost complete colocalization of CALM with AP-2. In contrast, no significant colocalization of CALM with AP-1 was found. Thus, the plasma membrane–coated pits and vesicles are the main site of localization of CALM in the cell.

To assess the relative size of the cytosolic and membrane pools of CALM, we permeabilized the cells mildly with saponin to allow the release of cytosolic proteins from the cell. The cytosol (saponin extract) contained only a small

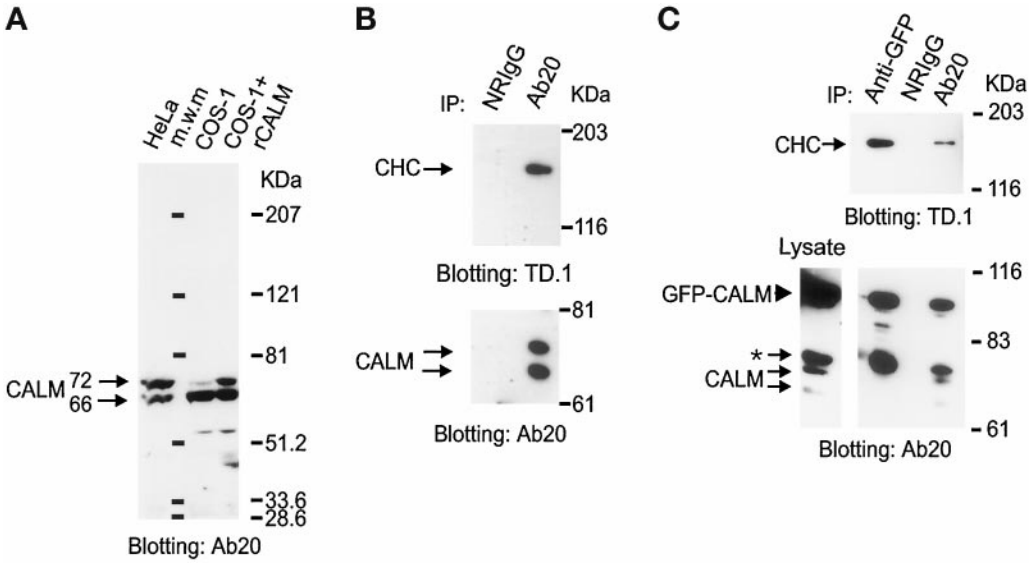

Figure 1. Western blotting detection and immunoprecipitation of CALM protein. (A) TX100 lysates of HeLa and COS-1 cells and of COS-1 cells transiently overexpressing CALM (COS-1 + rCALM) were resolved on 7.5% SDS-PAGE, and CALM was detected by blotting with Ab20. Molecular weight markers (m.w.m.) are indicated. (B) CALM protein was precipitated with Ab20 from TX100 lysates of HeLa cells, and the immunoprecipitates (IP) were analyzed by SDS-PAGE and Western blotting with Ab20 to CALM and antibody TD.1 to CHC. Nonspecific rabbit IgG (NRIgG) was used to control the specificity of immunoprecipitation. (C) The lysates of HeLa cells transfected with GFP fused to full-length CALM (GFP–CALM) were incubated with anti-GFP, Ab20, or nonspecific IgG, and the immunoprecipitates were analyzed by electrophoresis and Western blotting with TD.1 or Ab20 to detect CHC or endogenous CALM and GFP–CALM, respectively. The positions of endogenous 72- and 66-kDa species of CALM and CHC are indicated by arrows. Note, significant overexpression of GFP–CALM (99 kDa) is indicated by the large arrow. The asterisk marks the proteolytic product of GFP–CALM (~74 kDa). A relatively high amount of the proteolytic product of GFP–CALM is found in immunoprecipitates, presumably, because of the proteolysis during the immunoprecipitation procedure.

pool of CALM (5–15%), whereas a large fraction of cellular CHC (40–60%) was released from permeabilized cells (Figure 4). The bulk of CALM was associated with the membrane fractions soluble and insoluble in TX100. Interestingly, the relative distribution of CALM in cellular fractions mirrors the distribution of AP-2 but not of AP-1 that is completely released by TX100 (Figure 4A). The immunofluorescence labeling of cells treated with saponin and TX100 reveals the punctate staining of CALM, AP-2 (Figure 4B), and clathrin (our unpublished data), suggesting that a pool of plasma membrane–coated pits is resistant to TX100 membrane solubilization.

To estimate the amount of CALM present in different cellular fractions relative to the amount of CHC, quantitative Western blot analysis was performed. As standards for immunodetection with antibody TD.1 to CHC and Ab20 to CALM, the GST-fused TD domain of CHC and the fragment 1–413 of CALM, respectively, were used. These quantitations revealed that CALM is present at near stoichiometric amounts relative to clathrin in TX100-soluble and -insoluble fractions. Because of the contribution of the components of TGN-derived clathrin-coated buds to the TX100-soluble fraction, the molar ratio of CALM to clathrin in endocytic-coated vesicles present in this fraction could be underestimated. A large pool of components of plasma membrane–coated vesicles is insoluble in TX100 (Figure 4, A and B) (references in Woodward and Roth, 1978; Goud *et al.*, 1985). Therefore, the molar ratio of CALM and clathrin in this fraction may provide a better estimate of the CALM/CHC ratio in the plasma membrane–coated pits and vesicles in vivo. Altogether, the data of Figures 3 and 4 indicate that CALM is a major component of the endocytic clathrin-coated pits.

Protein–Protein Interactions of CALM

To determine the major binding partners of CALM, we labeled HeLa cells metabolically with [^{35}S]methionine and incubated the cytosolic (saponin-extractable) and membrane (TX100- and sodium deoxycholate–soluble) fractions of the cells with GST–CALM immobilized on glutathione-agarose. The only protein that was specifically bound to GST–CALM in both cellular fractions has an apparent molecular mass of ~175 kDa (Figure 5A). Western blotting of the same membrane with the anti-CHC revealed that the CHC band precisely overlaps with the radioactive band (Figure 5A). The same protein was pulled down from the cytosol by the C-terminal fragment of CALM, GST–414–652. However, GST–414–652 did not precipitate CHC from the membrane fraction (Figure 5B). The N-terminal GST fusion GST–1–413 did not bring down any CHC. These data suggest that clathrin is the major binding partner of CALM. Binding involves primarily the C-terminal sequences of CALM, but the full-length protein is required for the full capacity of CALM to bind clathrin from cell lysates.

The binding of CALM to Eps15 homology (EH) domains is predicted because CALM has two NPF motifs (Salcini *et al.*, 1997; Wendland and Emr, 1998). However, no Eps15 or

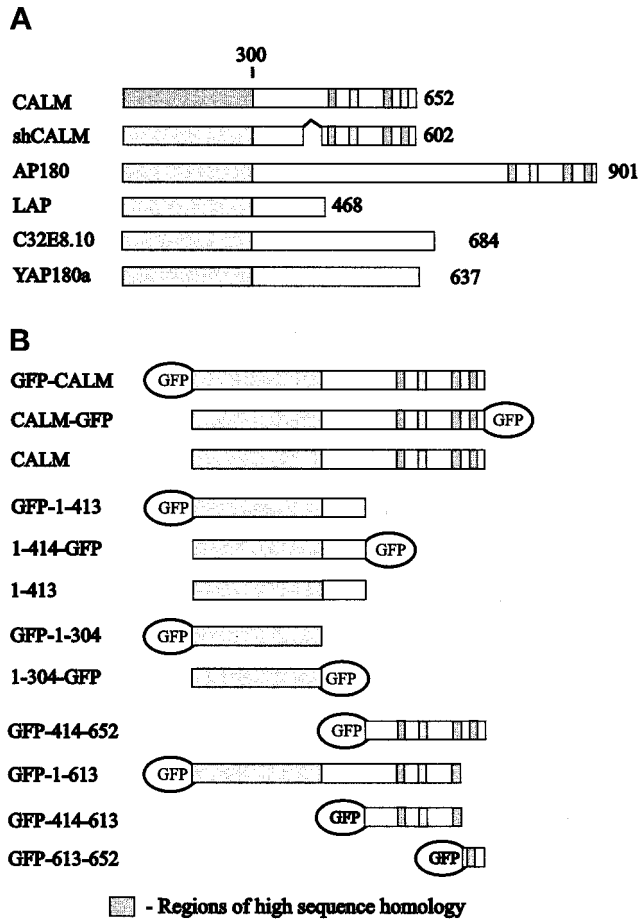

Figure 2. Schematic representation of CALM and homologous proteins. (A) Depicted are the full-length and the short-form human CALM (shCALM; 50 residues are deleted), rat AP180, *Drosophila melanogaster* LAP, *Caenorhabditis elegans* C32E8.10 (U88308), and yeast yAP180A. The approximate positions of the regions with the highest sequence similarity between proteins, corresponding to the CALM amino acid residues 1–300, 507–533, 539–553, 567–590, and 623–638, and the internal deletion of residues 420–469 (marked with ∧) because of the alternative splicing of human CALM are indicated. The number to the right of each lane represents the total number of residues. (B) The fragments of CALM expressed as GFP fusion proteins are shown. The first and the last CALM residues and the position of the GFP moiety are indicated for each construct. Fragments 1–413 and 414–652 as well as the full-length CALM were also expressed as GST fusion proteins.

Eps15R was detected by Western blotting in GST–CALM or GST–414–652 precipitates in experiments similar to one presented in Figure 5. No coimmunoprecipitation of Eps15 and CALM was observed in experiments similar to that described in Figure 1. Therefore, CALM either does not bind the EH domains of Eps15 at all or binds these domains very weakly.

The association of AP-2 with AP180 was observed previously in in vitro experiments and by coimmunoprecipitation (Kohtz and Puszkin, 1988; Wang *et al.*, 1995). Small amounts of α-adaptin (1–2% of the total cellular pool) were pulled down by GST–CALM and GST–414–652 from the cytosol and coimmunoprecipitated with CALM in TX100 cell lysates (our unpublished data).

A putative 65-kDa protein was pulled down from the cytosol by the GST–414–652 fragment but not by the full-length CALM. A protein with an apparent mass of 49 kDa was pulled down from the membrane fraction by GST–CALM but was not precipitated by its fragments. Bands corresponding to 48 and 40 kDa were apparently precipitated by the full-length and N-terminal part of CALM (Figure 5B). The identity of these proteins is unknown. Several other proteins were found in precipitates of full-length and nonoverlapping fragments of CALM and likely result from nonspecific interactions. There was no single band that is present in all pull-down precipitates containing CHC and is absent in precipitates of GST–1–413, suggesting that the interaction of CALM with clathrin is not mediated by another protein.

Cellular Localization of GFP–CALM

To study the distribution of CALM in living cells and to perform structure–function analysis of CALM, we expressed GFP–CALM transiently in COS-1 cells. The GFP localization and the effects of protein expression on the endocytosis of receptors were analyzed using digital-imaging microscopy. We have chosen COS-1 cells as the expression system, because they are easy to transfect, flattened on the plastic substrate, and are convenient for the light microscopy and for the measurement of transferrin and EGF receptor internalization. Figure 6A shows that GFP–CALM is diffusely distributed within the cytoplasm of living COS-1 cells and is also associated with small dots clearly seen at the cell periphery. In addition, there was an accumulation of GFP–CALM in the juxtanuclear area, typical of the Golgi complex, that consisted of several bright dots and diffuse fluorescence. To test whether the punctate fluorescence corresponds to the clathrin-coated pits and vesicles, double-label immunofluorescence studies were performed on formaldehyde-fixed cells. When moderately expressed in COS-1 cells, GFP–CALM is seen in dots throughout the cell and in the Golgi area and also associated with the edges of the cells (Figure 6B). The cytosolic diffuse fluorescence of GFP–CALM was less intense than that in living cells, presumably, because of the loss of GFP–CALM during cell permeabilization. Optical sectioning and digital deconvolution analysis revealed that the dots of GFP–CALM were often colocalized with CHC, suggestive of GFP–CALM localization at the plasma membrane–coated pits (Figure 6). Although CHC and GFP–CALM were seen accumulated in the same Golgi area, it was impossible to determine by light microscopy whether GFP–CALM is colocalized with the clathrin buds in the TGN. Peripheral diffuse staining and the staining of the cell edges probably correspond to cytosolic GFP–CALM and GFP–CALM associated with the plasma membrane. The colocalization of GFP–CALM with AP-2 in plasma membrane–coated pits was also clearly seen in double-labeled cells (our unpublished data). When GFP–CALM was highly overexpressed, the fluorescence of individual coated pits was difficult to distinguish on the background of the intense cytosolic or membrane fluorescence of GFP–CALM. Transfected CALM–GFP (GFP is at the C terminus; see Figure 2) and untagged CALM were found in the same locations as GFP–CALM (our unpublished data). However, the level of ex-

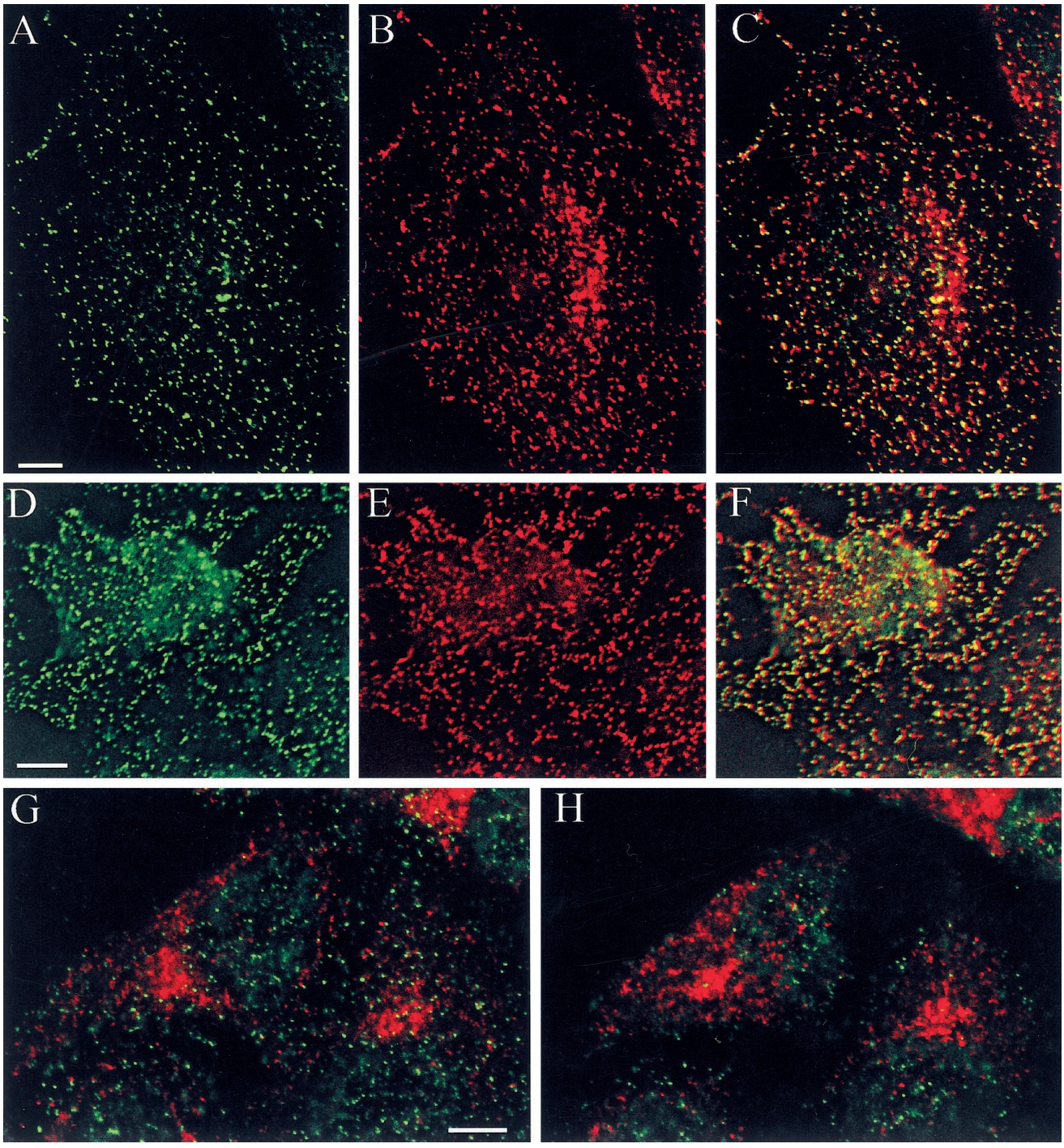

Figure 3. Localization of CALM in the cell. HeLa cells fixed with methanol (A–C) or methanol/acetone (D–H) were incubated with Ab20 and either X.22 (A–C), AP.6 (D–F), or 100/3 (G and H) monoclonal antibody followed by secondary anti-rabbit and anti-mouse IgG conjugated with fluorescein or CY3, respectively. The serial optical sections were acquired through the CY3 (red) and FITC (green) channels and deconvoluted as described in MATERIALS AND METHODS. The fluorescein and CY3 images representing individual optical sections (thickness of 0.2 μm) were merged (C, F, G, and H) after adjustment of both fluorescence signals to similar levels. The red images in C and F were shifted to the right by 3 pixels (0.2 μm), relative to green images to allow better visualization of the colocalization. Images in G and H represent two optical sections of the Z-stack that were acquired 3.6 μm apart. Bars: A–C, D–F, and G and H, 5 μm.

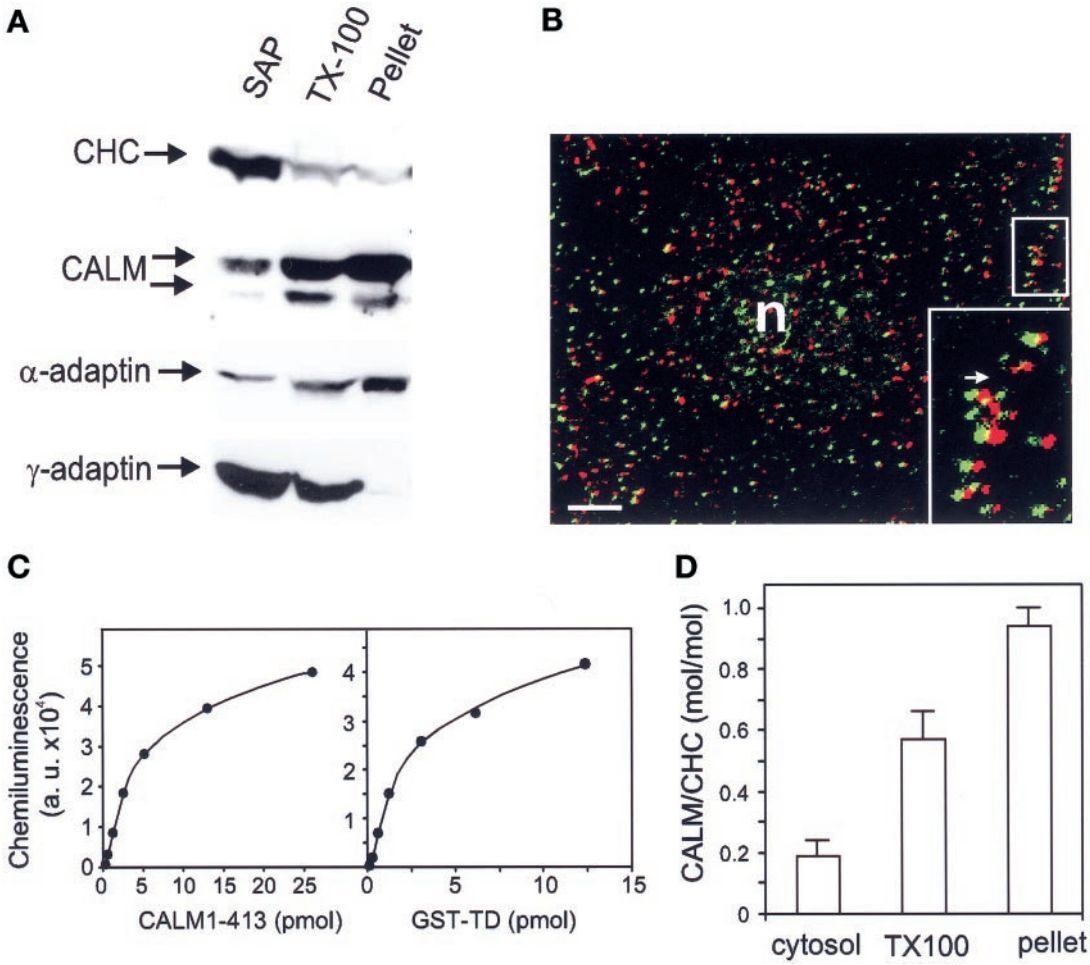

Figure 4. The quantitative analysis of CALM and CHC in cellular fractions. (A) The saponin (SAP) and TX100-soluble (TX-100) and -insoluble (pellet) fractions were obtained from HeLa cells as described in MATERIALS AND METHODS and resolved on SDS-PAGE. CHC, CALM, α-adaptin, and γ-adaptin were detected by Western blotting with antibodies TD.1, Ab20, AC.1, and 100/3, respectively. (B) HeLa cells grown on coverslips were permeabilized with saponin and TX100 as described in MATERIALS AND METHODS, fixed with methanol/acetone, and incubated with Ab20 and AP.6 followed by secondary anti-rabbit and anti-mouse IgG conjugated with fluorescein or CY3, respectively. The serial optical sections were acquired through the CY3 (red) and FITC (green) channels and deconvoluted. The fluorescein (CALM) and CY3 (AP-2) images representing individual optical sections (thickness of 0.2 μm) were merged, and the red image was shifted to the right by 3 pixels (0.2 μm) relative to the green image to allow better visualization of the colocalization. Inset (bottom right), high magnification of a group of coated pits (area indicated by white rectangular box) is shown; the arrow indicates the direction of the shift. The position of the nucleus is indicated (n). Bar, 5 μm. (C) Various amounts of CALM–1–413 and GST–TD were electrophoresed and blotted with, correspondingly, Ab20 and TD.1 simultaneously with the blotting of CALM and clathrin in cellular fractions obtained as described in A. Exemplary curves of the dependence of the chemiluminescence signals on the amount of proteins are presented. Typically, the intensity of these signals measured by densitometry (see MATERIALS AND METHODS) displayed linear dependence within the range of 1–5 pmol of the proteins. Arbitrary units (a.u.) represent the optical density units. (D) Various aliquots of HeLa cellular fractions were immunoblotted as described in A, and the chemiluminescence signals that fit within the linear range of the detection in the same experiments were used to calculate the mole/mole ratio of CALM and CHC. The data are averaged from four experiments similar to that presented in A. Error bars represent SDs.

pression of these proteins was at least a magnitude lower than the expression level of GFP–CALM. Apparently, the attachment of GFP to the N terminus stabilizes CALM.

To examine which part of CALM is responsible for targeting to clathrin-containing structures, we expressed GFP–1–413 and GFP–414–652 fragments (Figure 2) in COS-1 cells. GFP–414–652 displays a similar pattern of distribution in living and fixed COS-1 cells. Visual inspection of living cells suggests that the intensity of punctate fluorescence of GFP–414–652 (Figure 6E) is somewhat lower compared with that of GFP–CALM (Figure 6A). Figure 6, F–H, shows characteristic colocalization of GFP–414–652 in the structures containing clathrin. In contrast, the GFP–1–413 fragment is seen evenly distributed within the cell, with a stronger fluorescence signal associated with the areas of "thicker" cytoplasm, for instance, in the perinuclear area (Figure 6I). No

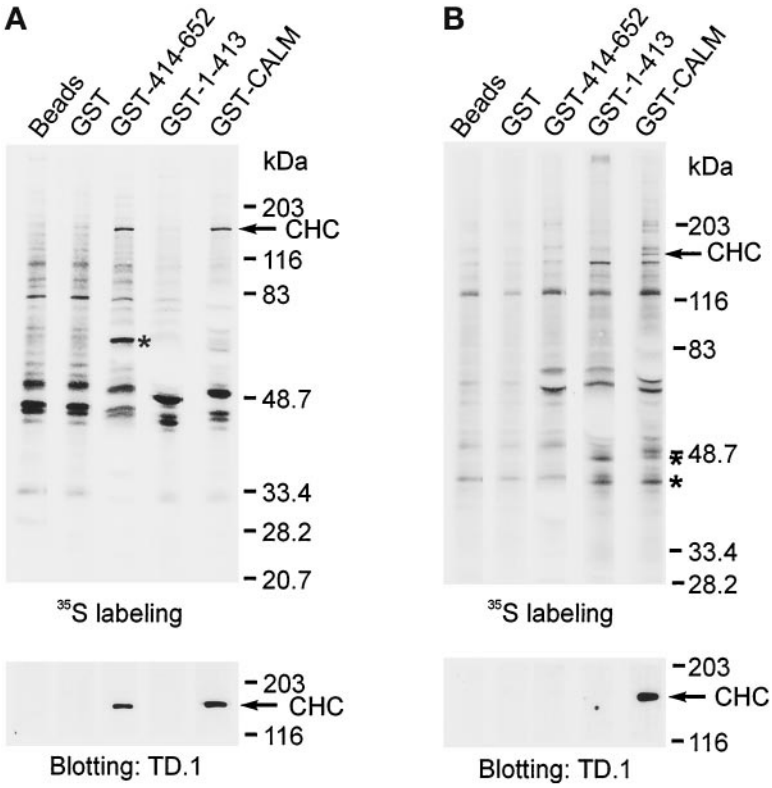

Figure 5. Binding of clathrin heavy chain to GST–CALM. GST–CALM, GST–1–413, and GST–414–652 were bound to glutathione-agarose beads and incubated with the cytosolic (saponin extract; A) or membrane (TX100 and deoxycholate extract; B) fractions of ^{35}S-metabolically labeled HeLa cells. Beads alone or with immobilized GST were used to control for the nonspecific binding of proteins. The agarose precipitates were resolved via 7.5% SDS-PAGE and transferred to a nitrocellulose membrane. Top, autoradiographs of the membranes are presented. The position of a 175-kDa–labeled band specifically associated with GST–CALM and GST–414–652 is indicated by arrows. Bottom, the same membranes were probed by Western blotting with antibody TD.1 to CHC. The detected band precisely overlapped with the 180-kDa radioactive band. The blots are from the same experiment. Asterisks mark other unidentified bands specifically bound to the fusion proteins.

punctate fluorescence in living cells and no obvious localization of this fragment in the plasma membrane–coated pits in fixed cells were observed (Figure 6, J–L). Essentially the same pattern of fluorescence was seen in the cells transfected with GFP alone (our unpublished data).

The fragment 1–413 contains domain 1–300 that is highly conserved in the AP180 protein family (Figure 2). The corresponding fragment of AP180 can bind to clathrin triskelions in vitro (Ye and Lafer, 1995a). The inability of the fragment 1–413 to be targeted to coated pits (Figure 6) and to bind clathrin in pull-down experiments (Figure 5) could be attributable to the GFP or GST moiety at the N terminus or additional residues 300–413 at the C terminus of the fragment. Therefore, fragments 1–413–GFP, 1–413, GFP–1–304, and 1–304–GFP (see Figure 2) were expressed in COS-1 cells. Untagged fragment 1–304 was not used because we do not have the antibody that recognizes this fragment. All these fragments displayed a diffuse pattern of staining similar to that of GFP–1–413, and none colocalized with AP-2 (our unpublished data). These data indicate that the N-terminal–conserved domain of CALM is not sufficient for targeting to the coated pits.

Effects of GFP–CALM Expression on Clathrin-mediated Receptor Traffic

Because CALM is localized to clathrin-coated pits, we sought to assess the role of CALM in clathrin-mediated endocytosis. Specifically, the effect of overexpression of full-length CALM and its fragments on the uptake of TRF–TR, a marker of coated pit–dependent internalization, was studied. Inspection of the population of cells transiently expressing GFP–414–652, a fragment that binds clathrin, revealed that a large proportion of the cells containing high levels of the fusion protein do not efficiently internalize TRF–TR as judged by the absence of TRF–TR accumulation in the juxta-Golgi area and peripheral endosomes (Figure 7, A and B). Similarly, endosomal TRF–TR was not seen in cells overexpressing GFP–CALM. The percent of cells in which endocytosis was inhibited was calculated as described in MATERIALS AND METHODS. Whereas 80 ± 7% (SD) of cells overexpressing GFP–CALM or GFP–414–652 displayed impaired endocytosis, this value was 8 ± 3% (SD) in cells expressing low or moderate amounts or not expressing these proteins. Fragment GFP–1–613 also imposed a dominant-negative effect on endocytosis. In contrast, there was no significant effect of overexpression of GFP–1–413 on transferrin endocytosis (Figure 7, G and H). The expression of 1–413–GFP, GFP–1–303, 1–303–GFP, and 1–413 also did not affect the endocytosis of TRF–TR. The percent of inhibition in cells expressing fragments of the N terminus of GFP alone at the level comparable with that of GFP–CALM was within the range of 4–20%.

The EGF-activated EGF receptor is also internalized by the clathrin-mediated pathway, although EGF receptors do not compete with transferrin receptors for the same saturable element of the internalization machinery (Warren *et al.*, 1998). The uptake of the EGF–Texas Red conjugate was inhibited in COS-1 cells overexpressing GFP–CALM and GFP–414–652 (our unpublished data). To demonstrate this effect in an independent quantitative assay, we measured

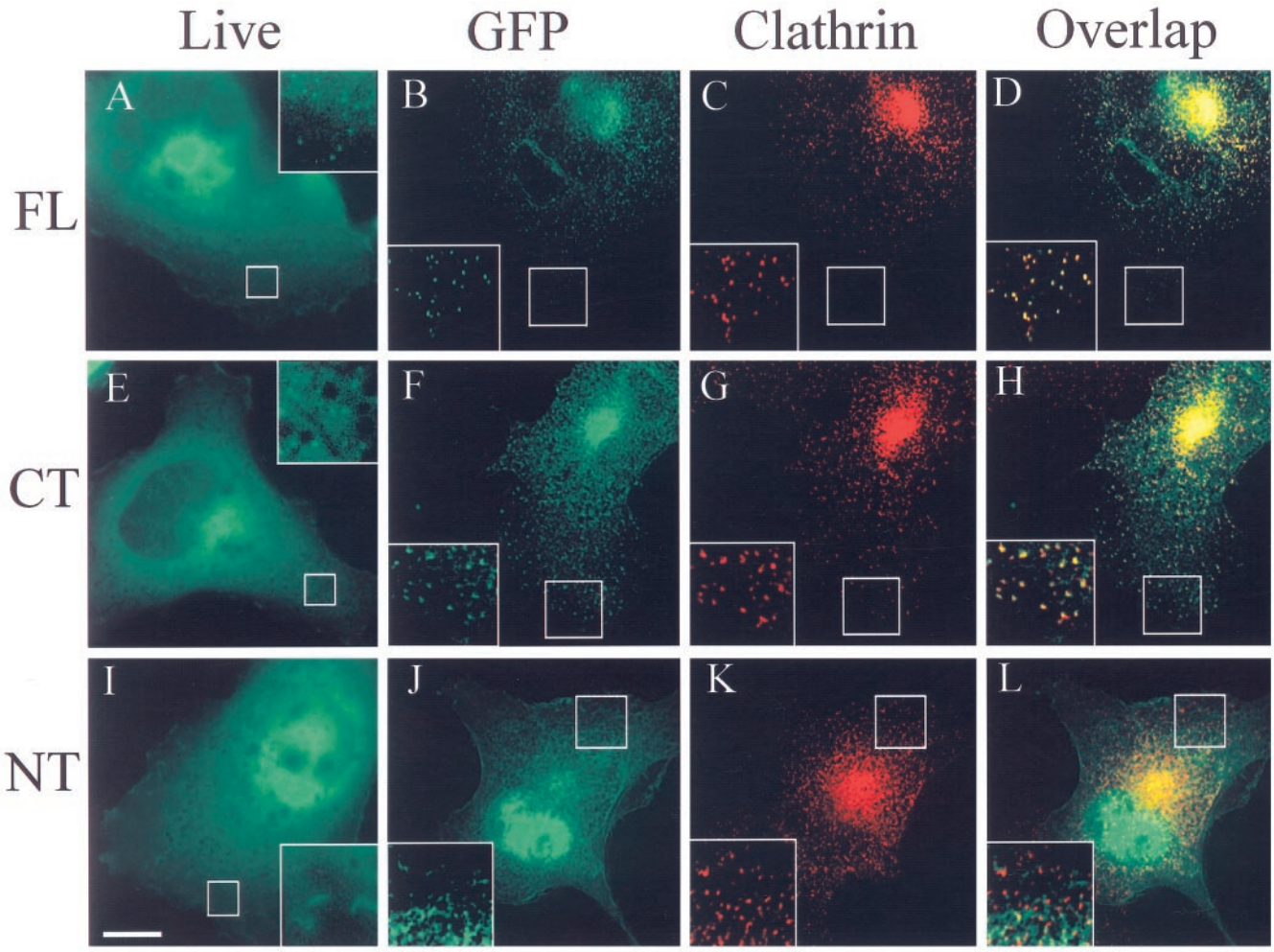

Figure 6. The localization of GFP–CALM in living and fixed cells. COS-1 cells were transiently transfected with GFP–CALM (FL; A–D), GFP–414–652 (CT; E–H), or GFP–1–413 (NT; I–L). (A, E, and I) For living-cell microscopy, cells were grown in microscope chambers, and the images were acquired through the GFP channel as described in MATERIALS AND METHODS. (B–D, F–H, and J–L) Cells grown on coverslips were fixed and stained with antibody X.22 to CHC followed by secondary IgGs labeled with Texas Red. The serial optical sections were acquired through the Texas Red (red) and GFP (green) channels and deconvoluted as described in MATERIALS AND METHODS. The fluorescein (green) and Texas Red (red) channels were merged (D, H, and L) after adjustment of both fluorescence signals to similar levels. Yellow indicates the overlap of Texas Red and fluorescein fluorescence. All images comprise an individual optical section. Insets, the peripheral regions of the cells indicated by white square boxes are shown at higher magnification and with enhanced contrast. Bar, 5 μm.

the rates of ^{125}I-labeled EGF internalization in cells transiently transfected with CALM or its fragments. Figure 8 shows that overexpression of full-length GFP–CALM and GFP–414–652 results in significant inhibition of ^{125}I-labeled EGF uptake. Because no more than one-half of the cell population express GFP–CALM or GFP–414–652 at levels sufficient to block coated-pit endocytosis, the rate of EGF internalization in cells overexpressing GFP-fused proteins could be projected to be as low as the minimal internalization rate for EGF receptor mutants incapable of clathrin-dependent internalization (Sorkin *et al.*, 1992). Expression of GFP–1–413 (Figure 8) or GFP–1–304 (our unpublished data) did not result in any inhibition of endocytosis compared with that in the mock-transfected cells. Because the fragments fused with GFP at the C terminus or not tagged did not express at high levels in a large pool of cells, these fragments were not tested in the ^{125}I-labeled EGF internalization assay. Together, the data in Figures 7 and 8 demonstrate that overexpression of CALM or its fragments, containing the clathrin interaction portion, significantly inhibits receptor-mediated endocytosis.

GFP–CALM and Clathrin in TGN

Clathrin-dependent protein trafficking also occurs at the TGN. The multilabel fluorescence analysis of clathrin staining of transfected COS-1 cells showed that in many cells overexpressing GFP–CALM or GFP–414–652 the normal aggregation of clathrin immunoreactivity at the TGN is not seen (Figure 7, C and F). The effect of GFP fusion overex-

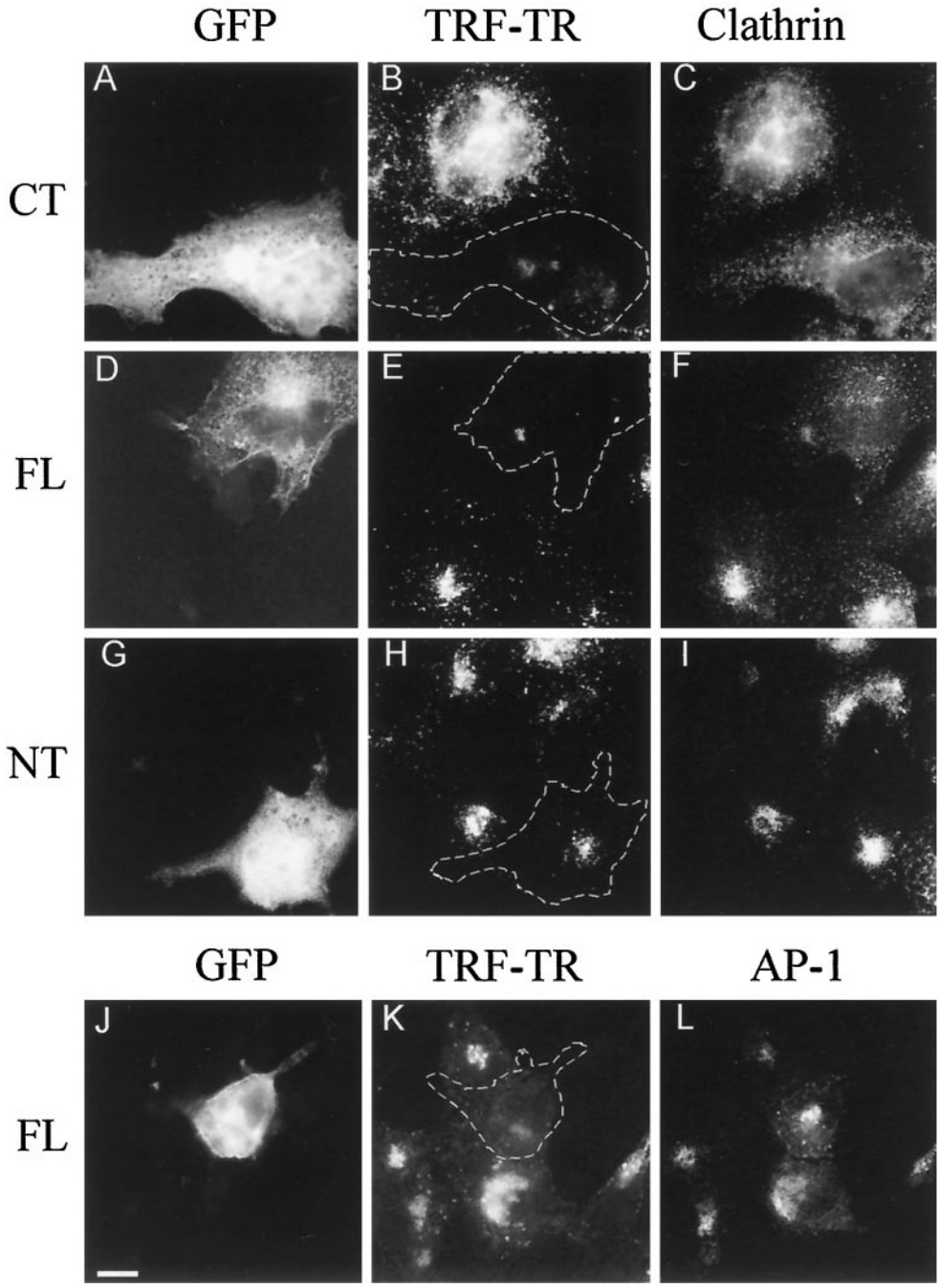

Figure 7. The effect of GFP–CALM overexpression on transferrin endocytosis and clathrin distribution. COS-1 cells expressing GFP–414–652 (CT; A–C), GFP–CALM (FL; D–F and J–L), or GFP–1–413 (NT; G–I) were incubated with 5 μg/ml TRF–TR for 15 min at 37°C, fixed, and stained with antibodies X.22 to CHC (A–I) or 100/3 to γ-adaptin (J–L) followed by secondary IgGs labeled with AMCA. The serial optical sections were acquired through the Texas Red (red), GFP (green), and AMCA/DAPI (blue) channels and deconvoluted as described in MATERIALS AND METHODS. All images represent the merged images of 20 serial optical sections (total thickness of 4 μm). The approximate perimeter of GFP-expressing cells is indicated in the images of TRF–TR endocytosis by the dashed lines (B, E, H, and K). Bar, 5 μm.

pression on TGN-associated clathrin correlated well with the inhibition of TRF–TR endocytosis. In contrast, GFP–1–413 did not redistribute clathrin from the TGN (Figure 7H). The localization of clathrin in cells overexpressing GFP–CALM is shown in more detail in Figure 9, A and B. In many cells the dispersion of the TGN-associated clathrin staining

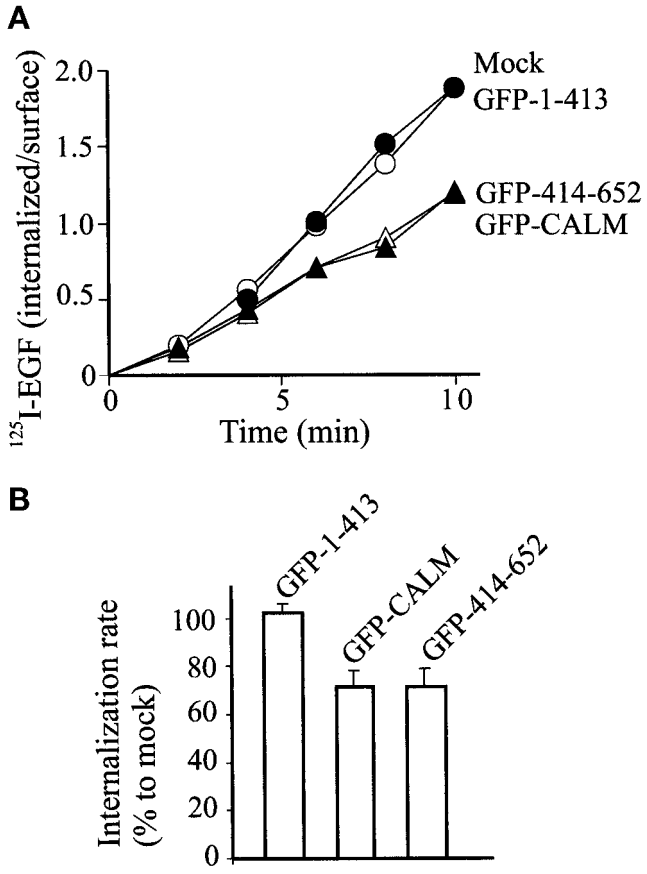

Figure 8. Internalization of ^{125}I-labeled EGF in GFP–CALM–expressing cells. (A) COS-1 cells transfected with GFP (mock; ○), GFP–CALM (▲), GFP–414–652 (△), or GFP–1–413 (●) were incubated with 2.0 ng/ml ^{125}I-labeled EGF for 1–10 min, and the amount of surface-bound and internalized radioactivity was determined as described in MATERIALS AND METHODS. The rate of internalization is expressed as the ratio of internalized and surface ^{125}I-labeled EGF for each time point. (B) Internalization rates are averaged from four experiments performed as described in A. The rates are expressed as the percent of internalization rates in mock-transfected cells.

was coincident with the appearance of large structures containing clathrin in the perinuclear area.

The release of clathrin from the TGN did not appear to disrupt the TGN-associated accumulation of GFP–CALM or GFP–414–652 in the TGN area. Importantly, the overexpression of these proteins did not lead to redistribution of AP-1 from the TGN (Figure 7, J–L). These data suggest that the integrity of the TGN is not affected by GFP–CALM overexpression whereas the recruitment of clathrin to TGN membranes and the clathrin–AP-1 interactions are abrogated.

To assess whether the dramatic loss of clathrin from the TGN membranes affects the protein traffic through TGN-coated pits, we inspected the subcellular distribution of the cation-independent M6P receptor, which uses the clathrin-mediated pathway from the TGN to endosomes (Traub and Kornfeld, 1997). Immunofluorescence staining of COS-1 cells detected most M6P receptors in large endosome-like organelles in the perinuclear area and a small pool of receptors in the TGN. Interestingly, overexpression of GFP–CALM significantly diminished the endosomal staining of the M6P receptor (Figure 9, C and D), suggesting that receptor movement from the TGN and presumably the cell surface to endosomes is inhibited. A similar effect was observed in cells overexpressing GFP–414–652 (Figure 9, E and F), whereas GFP–1–413 did not have any effect on M6P receptor localization (our unpublished data). Taken together, the data presented in Figures 7–9 demonstrate that overexpression of the clathrin-binding fragment of CALM or full-length CALM impairs two major clathrin-mediated trafficking processes occurring at the cell surface and at the TGN. Thus, GFP–CALM and its fragments may serve as useful tools for comparative studies of the role of clathrin in the trafficking of the variety of the proteins, lipids, and viruses at the cell surface and TGN as well as in other compartments such as endosomes and secretory granules.

Interactions of CALM with Clathrin In Vivo

The effect on receptor endocytosis and clathrin–AP-1 interaction at the TGN can be explained if the overexpression of GFP–CALM or its C-terminal portion disrupted the protein–protein interactions involved in clathrin vesicle formation. Our results show that clathrin is the major CALM-binding partner. To test whether GFP–CALM expressed in COS-1 cells forms complexes with clathrin retained during cell solubilization, a coimmunoprecipitation assay was used. GFP–CALM and CHC were immunoprecipitated from TX100 cell lysates with anti-GFP and anti-CHC (X.22) antibodies, respectively. GFP and CHC were then probed in the immunoprecipitates by Western blotting (Figure 10A). Both reciprocal coimmunoprecipitations indicated the presence of GFP–CALM–CHC complexes. The pools of CALM and CHC insoluble in TX100 could be released by sodium deoxycholate (1%). However, deoxycholate treatment resulted in a poor immunoprecipitation efficiency of anti-GFP and abolished the interaction of CALM fragment GST–413–652 with CHC in vitro (Figure 5 and our unpublished data). Therefore, we were not able to determine the extent of CHC–CALM association in the TX100-insoluble fraction.

To map the region of CALM involved in the interaction with CHC, we expressed various parts of CALM as GFP fusion proteins in COS-1 cells. Immunoprecipitation with anti-GFP revealed that CHC is significantly bound to GFP–413–652 but not to GFP–1–413 (Figure 10B). The smaller fragments of the N terminus such as GFP–1–304 (Figure 10B) and 1–304–GFP (our unpublished data) also did not coimmunoprecipitate CHC.

The ability of GFP–414–652 to bind clathrin correlated with its inhibitory effect on clathrin-mediated trafficking (Figures 7–9). Two parts of the C terminus, GFP–414–613 and GFP–613–652 (Figure 2), each containing sequences highly homologous to rat brain AP180, were expressed in COS-1 cells, and their ability to interact with CHC was examined using coimmunoprecipitation. Figure 10B shows that neither fragment was associated with clathrin to a significant extent, although clathrin binding of the GFP–414–613 fragments was detected in several experiments. These data suggest that both regions are necessary for the efficient interaction of GFP–414–652 with CHC. Surprisingly, the large fragment of CALM, GFP–1–613 (see Figure 2) that

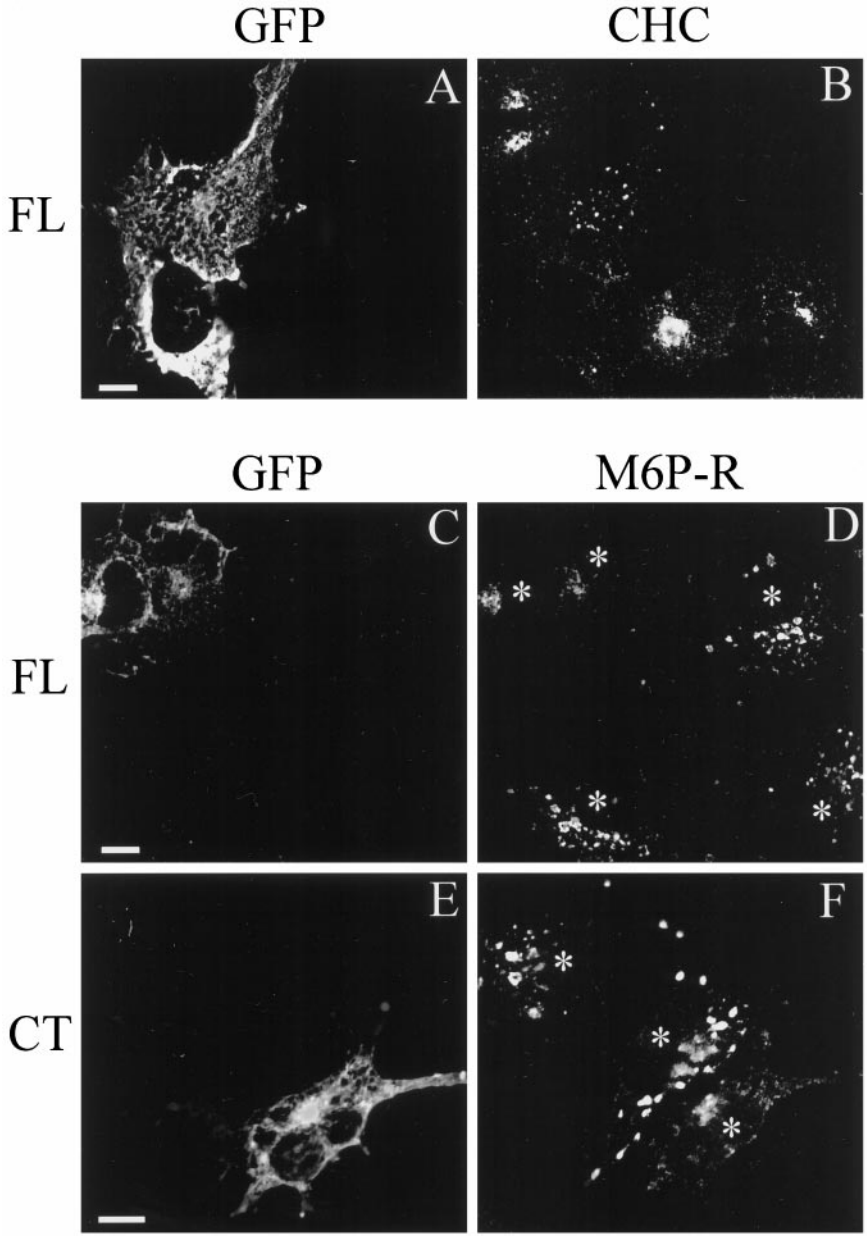

Figure 9. The effect of GFP–CALM expression on the localization of clathrin and M6P receptor. COS-1 cells expressing GFP–CALM (FL; A–D) or GFP–414–652 (CT; E and F) grown on coverslips were fixed and stained with mouse monoclonal anti-clathrin X.22 (A and B) and rabbit polyclonal anti-M6P receptor (C–F) followed by the secondary goat IgGs specific to mouse or rabbit IgG, respectively, labeled with Texas Red. The serial optical sections were acquired through the Texas Red (red) and GFP (green) channels and deconvoluted as described in MATERIALS AND METHODS. Images represent the merged images of two serial optical sections (total thickness of 0.4 μm) from the middle of the cell, where the most intense signal for CHC or M6P receptor (M6P-R) in the perinuclear area was observed. Asterisks show the position of cell nuclei. Bars: A and B, C and D, and E and F, 10 μm.

lacks the fragment 614–652, could efficiently coimmunoprecipitate CHC (Figure 9B). This result suggests that in the presence of the N-terminal portion of CALM, the small region 614–652 is not required for the interaction with clathrin. It should be noted that the absolute amounts of coimmunoprecipitated CHC and GFP–CALM or its fragments varied in different experiments because of variability in the transfection efficiencies and the resulting cytosol/membrane distribution of GFP-fused proteins.

Overall, the ability of GFP fusion fragments of CALM to bind clathrin strongly correlated with their localization in clathrin-coated pits and vesicles and with the inhibitory effect on endocytosis when overexpressed. In all assays, full-length CALM displayed the highest capability to bind clathrin. Together, the data of GST pull-down and coimmunoprecipitation experiments suggest that CALM has several clathrin-binding interfaces and that possibly two of them are located within the C-terminal region 414–652.

DISCUSSION

The experiments performed in this study provide the first characterization of the biochemical and functional properties of CALM, a new component of the clathrin coat in nonneuronal cells. CALM is homologous to the brain-specific protein AP180, and the rationale of many experiments in this study was based on what is known about AP180.

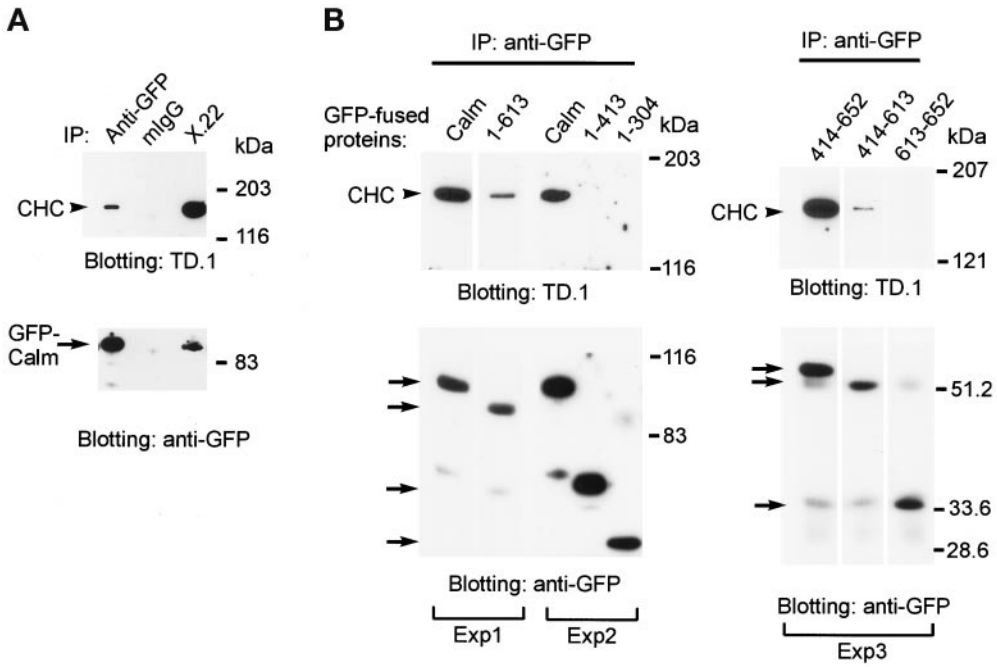

Figure 10. Coimmunoprecipitation of CHC with CALM and its fragments. (A) The lysates of COS-1 cells transfected with GFP–CALM were incubated with anti-GFP, X.22, or nonspecific mouse IgG (mIgG), and the immunoprecipitates were resolved by SDS-PAGE. CHC and GFP–CALM were detected by blotting with TD.1 or anti-GFP, respectively. (B) GFP–CALM, GFP–414–652, GFP–1–413, GFP–1–304, GFP–1–613, GFP–414–613, and GFP–613–652 fragments (see Figure 2) were immunoprecipitated with anti-GFP from the TX100 lysates of transiently transfected COS-1 cells. The immunoprecipitates were analyzed by SDS-PAGE, and the presence of CHC and GFP fusion proteins in the immunoprecipitates was detected by blotting with antibodies TD.1 or anti-GFP, respectively. Arrows indicate the positions of the GFP fusion proteins, whereas the arrowheads point to the position of CHC. The lanes in each panel (labeled Exp1, Exp2, and Exp3) are from the same experiment. The data in each panel are representative of several independent experiments.

Immunofluorescence labeling of CALM revealed the presence of this protein in all detectable coated pits at the cell surface, suggesting that CALM may play a role in a general step of clathrin-mediated endocytosis. CALM is coimmunoprecipitated with clathrin (CHC) in cell lysates and binds CHC in pull-down experiments. In the cell, CALM is present in a lower molar amount than is CHC. However, whereas a large pool of clathrin is found in the cytosol, the bulk of CALM is associated with the membrane and the detergent-insoluble fractions of the cell where it is present at near stoichiometric amounts relative to CHC. We suggest that the molar ratio of CHC to CALM in the TX100-insoluble fraction approximately corresponds to this ratio in plasma membrane–coated pits and vesicles. First, surface-coated pits appear to be the main and probably the only site of CALM localization in the cell. A pool of endocytic-coated pits and vesicles is resistant to TX100 extraction, whereas the majority of membrane-associated proteins including AP-1 are released by this detergent (Figure 4) (references in Woodward and Roth, 1978; Goud *et al.*, 1985). The punctate staining of AP-2 and clathrin remains clearly visible in cells treated with TX100 (Figure 4), whereas no AP-1 and clathrin are seen accumulated in the Golgi area (our unpublished data). A molar ratio of 1:1 was determined previously for AP180 and CHC in the brain-derived coated vesicle preparations. Thus, AP180 and/or CALM together with AP-2 and clathrin may be the structural elements of plasma membrane coats in neuronal and nonneuronal cells.

Studies of AP180 have described the clathrin-binding and coat-assembly activities of this protein in vitro in detail, although the mechanism of AP180 binding to clathrin remains unclear. Apparently, both N-terminal (33 kDa) and C-terminal (55 kDa) parts of AP180 have clathrin-binding activity (Ye and Lafer, 1995a,b). The N-terminal domain of AP180 is almost identical to the corresponding region of CALM that is also important for the full clathrin-binding capacity of CALM (Figure 10B). However, our data indicate that N-terminal fragments of CALM do not bind CHC in cell lysates and are not targeted to clathrin-coated pits regardless of whether the tag is at the N- or the C terminus or the fragment is not tagged. These data suggest that the potential ability of the 1–303 fragment to bind clathrin triskelions in vitro is not sufficient for interaction with clathrin in cell lysates, targeting to coated pits, and the dominant-negative effect on endocytosis. In contrast, the GFP-tagged C-terminal portion of CALM (residues 413–652 corresponding to the last 27-kDa portion of AP180) coimmunoprecipitates with clathrin under mild conditions and is localized to plasma membrane–coated pits. The important role of the C terminus of CALM in binding to clathrin is supported by the observation that yeast YAP180 binds to clathrin also via the C-terminal domain (Wendland and Emr, 1998).

It can be suggested that multiple interfaces participate in CALM–CHC interactions. At least two hydrophobic stretches within the C-terminal portion of CALM display high homology to rodent AP180 and could be responsible

for binding to CHC. However, the molecular details of the binding of CALM and/or AP180 and other proteins to CHC remain to be elucidated. A putative sequence consensus L (L, I) (D, E, N) (L, F) (D, E) has been suggested to participate in the protein binding to the TD domain of CHC (Dell'Angelica *et al.*, 1998). However, it is unlikely that this sequence is a general clathrin-binding consensus and is sufficient for the interaction with the TD domain. For instance, both nonvisual arrestins and AP-2 have this motif but do not compete for binding to the TD domain (Goodman *et al.*, 1997). The sequence LLDL (393–396), which resembles this clathrin-binding consensus, is situated within the 1–413 fragment that is incapable of interaction with clathrin in cell lysates (Figures 5 and 10). Although detailed mutagenesis studies are necessary to map precisely the sequence motifs involved, it is possible that the presence of at least two binding sites is required for stable interaction of CALM with clathrin. For instance, in the absence of the binding site in the fragment 613–652, the sequence(s) located in the N-terminal fragment 1–413 is required for clathrin binding of the fragment GFP–1–613 (Figure 10). On the other hand, two or more sites of interactions within the 414–652 fragment are sufficient for binding to CHC. It is also possible that all binding activity is located within the fragment 414–613, but the folding of this fragment fused to GFP does not allow its proper binding to CHC. In all types of assay, the full-length CALM displayed the greatest ability to localize to clathrin-containing organelles and to bind clathrin, consistent with the additivity of the clathrin-binding motifs.

The mechanism of the specific targeting of endogenous CALM to the plasma membrane is unclear. Binding to clathrin cannot be sufficient for this targeting because clathrin is present in other cellular organelles. In fact, when GFP–CALM is expressed at high levels, it is found in the Golgi area and cytosol in addition to its normal localization at the plasma membrane. It is possible that endogenous CALM is selectively recruited to the plasma membrane–coated pits via binding to AP-2. CALM has one DPF sequence within the fragment 414–652 (residues 420–422). DPF and DFW motifs have been implicated in the interaction with the C terminus of the α-subunit of AP-2 (Chen *et al.*, 1998). However, in our experiments very little AP-2 was detected in CALM immunoprecipitates and pull-downs. This pool of AP-2 could be bound to CALM indirectly via clathrin. It is also possible that DPF-based interactions are not strong enough to survive the conditions of our binding assays. Although the interaction of AP180 with α-adaptin was observed in vitro (Wang *et al.*, 1995), DPF motifs are not conserved in CALM homologous proteins. Therefore, it is unlikely that DPF–AP-2 interactions determine the localization of CALM in endocytic-coated pits. Another hypothetical possibility is that CALM can selectively interact with the plasma membrane–associated cytoskeleton or lipids.

Despite the presence of two NPF motifs, no interaction of CALM with Eps15 or Eps15R was detected in the GST pull-down and coimmunoprecipitation experiments. Because the NPF–EH interaction affinity is low (De Beer *et al.*, 1998), the CALM–EH complex may not be detectable in conventional protein–protein interaction assays. Denatured GST–CALM or GST–414–652 can bind the recombinant EH domains of Eps15 in a far Western assay (our unpublished data). The possibility exists that the localization of these proteins in close proximity in coated pits may allow a significant increase of local concentrations of EH domains and CALM, thus leading to the stable interaction of these proteins. It is also possible that CALM can bind to the EH domains of proteins other than Eps15, for instance to intersectin (Yamabhai *et al.*, 1998).

In summary, we identified only one interaction partner of CALM, the clathrin heavy chain. Whereas clathrin is probably the major interactor of the C-terminal domain of CALM, identification of binding partners for the conserved N-terminal domain is important for the elucidation of CALM function. However, analysis of CALM interactions in coated pits is difficult because the large pool of the mature clathrin-coated pits is insoluble under mild conditions. Solubilization in the presence of ionic detergents like sodium deoxycholate or high concentrations of salts dramatically weakens the interaction of CALM with clathrin (Figure 5) and probably other molecules.

Overexpression of GFP–CALM caused inhibition of endocytosis and disrupted clathrin localization in the TGN, thus affecting TGN–endosome trafficking. These two effects may have similar or different mechanisms. Endogenous CALM is located only in endocytic-coated pits. Therefore, the localization of GFP–CALM in the Golgi area and the effects of CALM on TGN may not be related to CALM function. Apparently, CALM prevents the recruitment of clathrin to the membrane-associated AP-1, which results in mistargeting clathrin. This could be the result of the competition for binding to CHC between CALM and AP-1. In contrast, overexpression of GFP–CALM or its clathrin-binding fragments did not cause any visible mistargeting effect on plasma membrane clathrin. Apparently, clathrin/AP-2 coats are more stable than clathrin/AP-1 coats. The stability of plasma membrane–coated pits can be illustrated by their resistance to detergent solubilization. CALM may have multiple binding sites on the CHC molecule as shown for AP180 (Murphy and Keen, 1992), and the association of an additional CALM with CHC may disrupt interactions of other proteins with clathrin within the preformed coat. Thus, the amount of CALM relative to that amount of clathrin and other components of coated pits might be an important regulator of the endocytosis process. A recent report describing the effect of knock-out of LAP in *Drosophila* implicates proteins of the CALM and/or AP180 family in the regulation of the size of the coated vesicles (Zhang *et al.*, 1998). By interacting with several sites of CHC, CALM can regulate the curvature of the coat and, therefore, the size of the budding vesicle. Future ultrastructure studies should determine whether overexpression of CALM affects the size of coated pits and vesicles in mammalian cells.

Thus, CALM may participate in the formation of the clathrin vesicle by regulating the interactions involving the TD and possibly other domains of CHC. Obviously, alternative models of CALM function can be proposed. For instance, CALM can potentially associate with phosphatidylinositols (Hao *et al.*, 1997) and provide an additional force for the recruitment of clathrin to the membrane. Finally, CALM may serve as an adaptor for recruitment of proteins into the coated pit. In this case the C-terminal domain of CALM would bind to the TD domain of CHC, whereas the N terminus of CALM would interact with the intracellular tail of cargoes.

ACKNOWLEDGMENTS

The authors thank Drs. Kathryn Howell, Randy Taylor, and Royston Carter for critically reading the manuscript. We are grateful to Dr. Macovcik for the gift of antibodies and Dr. J. Keen for the GST–TD plasmid. This work was supported by National Institutes of Health grant DK-46817 and a grant from the Cancer League of Colorado. Cancer Center Core facilities are supported by National Institutes of Health grant CA-46934.

REFERENCES

Ahle, S., and Ungewickell, E. (1986). Purification and properties of a new clathrin assembly protein. EMBO J. *5*, 3143–3149.

Brodsky, F.M. (1985). Clathrin structure characterized with monoclonal antibodies. I. Analysis of multiple antigenic sites. J. Cell Biol. *101*, 2047–2054.

Carpenter, G., and Cohen, S. (1976). ^{125}I-Labeled human epidermal growth factor: binding internalization, and degradation in human fibroblasts. J. Cell Biol. *71*, 159–171.

Chen, H., Fre, S., Slepnev, V.I., Capua, M.R., Takei, K., Butler, M.H., Di Fiore, P.P., and De Camilli, P. (1998). Epsin is an EH-domain-binding protein implicated in clathrin-mediated endocytosis. Nature *394*, 793–797.

De Beer, T., Carter, R.E., Lobel-Rice, K.E., Sorkin, A., and Overduin, M. (1998). Structure and Asn-Pro-Phe binding pocket of the eps15 homology domain. Science *281*, 1357–1360.

Dell'Angelica, E.C., Klumperman, J., Stoorvogel, W., and Bonifacino, J.S. (1998). Association of the AP-3 adaptor complex with clathrin. Science *280*, 431–434.

Dreyling, M.H., Martinez-Climent, J.A., Zheng, M., Mao, J., Rowley, J.D., and Bohlander, S.K. (1996). The t(10,11)(p13;q14) in the U937 cell line results in the fusion of the AF10 gene and CALM, encoding a new member of the AP-3 clathrin assembly protein family. Proc. Natl. Acad. Sci. USA *93*, 4804–4809.

Gill, S.C., and von Hippel, P.H. (1989). Calculation of protein extinction coefficients from amino acid sequence data. Anal. Biochem. *182*, 319–326.

Goodman, O.B., Jr., Krupnick, J.G., Gurevich, V.V., Benovic, J.L., and Keen, J.H. (1997). Arrestin/clathrin interaction. Localization of the arrestin binding locus to the clathrin terminal domain. J. Biol. Chem. *272*, 15017–15022.

Goud, B., Huet, C., and Louvard, D. (1985). Assembled and unassembled pools of clathrin: a quantitative study using an enzyme immunoassay. J. Cell Biol. *100*, 521–527.

Hao, W., Tan, Z., Prasad, K., Reddy, K.K., Chen, J., Prestwich, G.D., Falck, J.R., Shears, S.B., and Lafer, E.M. (1997). Regulation of AP-3 function by inositides. Identification of phosphatidylinositol 3,4,5-triphosphate as a potent ligand. J. Biol. Chem. *272*, 6393–6398.

Keen, J.H., and Black, M.M. (1986). The phosphorylation of coated membrane proteins in intact neurons. J. Cell Biol. *102*, 1325–1333.

Kohtz, D.S., and Puszkin, S. (1988). A neuronal protein (NP185) associated with clathrin-coated vesicles. Characterization of NP185 with monoclonal antibodies. J. Biol. Chem. *263*, 7418–7425.

Lindner, R., and Ungewickell, E. (1992). Clathrin-associated proteins of bovine brain coated vesicles. An analysis of their number and assembly-promoting activity. J. Biol. Chem. *267*, 16567–16573.

Murphy, J.E., and Keen, J.H. (1992). Recognition sites for clathrin-associated proteins AP-2 and AP-3 on clathrin triskelia. J. Biol. Chem. *267*, 10850–10855.

Murphy, J.E., Pleasure, I.T., Puszkin, S., Prasad, K., and Keen, J.H. (1991). Clathrin assembly protein AP-3. The identity of the 155K protein, AP180, and NP185 and demonstration of a clathrin binding domain. J. Biol. Chem. *266*, 4401–4408.

Norris, F.A., Ungewickell, E., and Majerus, P.W. (1995). Inositol hexakisphosphate binds to clathrin assembly protein 3(AP-3/AP180) and inhibits clathrin cage assembly in vitro. J. Biol. Chem. *270*, 214–217.

Odorizzi, G., Cowles, C.R., and Emr, S.D. (1998). The AP-3 complex: a coat of many colors. Trends Cell Biol. *8*, 282–288.

Robinson, M.S. (1997). Coats and vesicle budding. Trends Cell Biol. *7*, 99–102.

Salcini, A.E., Confalonieri, S., Doria, M., Santolini, E., Tassi, E., Minenkova, O., Cesareni, G., Pelicci, P.G., and Di Fiore, P.P. (1997). Binding specificity and in vivo targets of the EH domain, a novel protein-protein interaction module. Genes Dev. *11*, 2239–2249.

Schmid, S. (1997). Clathrin-coated vesicle formation and protein sorting: an integrated process. Annu. Rev. Biochem. *66*, 511–548.

Sorkin, A., Helin, K., Waters, C.M., Carpenter, G., and Beguinot, L. (1992). Multiple autophosphorylation sites of the epidermal growth factor receptor are essential for receptor kinase activity and internalization. J. Biol. Chem. *267*, 8672–8678.

Sorkin, A., Mazzotti, M., Sorkina, T., Scotto, L., and Beguinot, L. (1996). Epidermal growth factor interaction with clathrin adaptors is mediated by the Tyr974-containing internalization motif. J. Biol. Chem. *271*, 13377–13384.

Stoorvogel, W., Oorschot, V., and Geuze, H.J. (1996). A novel class of clathrin-coated vesicles budding from endosomes. J. Cell Biol. *132*, 21–33.

Takei, K., Mundigl, O., Daniell, L., and De Camilli, P. (1996). The synaptic vesicle cycle: a single vesicle budding step involving clathrin and dynamin. J. Cell Biol. *133*, 1237–1250.

Traub, L.M., and Kornfeld, S. (1997). The *trans*-Golgi network: a late secretory sorting station. Curr. Opin. Cell Biol. *9*, 527–533.

Wang, L.H., Sudhof, T.C., and Anderson, R.G. (1995). The appendage domain of alpha-adaptin is a high affinity binding site for dynamin. J. Biol. Chem. *270*, 10079–10083.

Warren, R.A., Green, F.A., Stenberg, P.E., and Enns, C.A. (1998). Distinct saturable pathways for the endocytosis of different tyrosine motifs. J. Biol. Chem. *273*, 17056–17063.

Wendland, B., and Emr, S.D. (1998). Pan1p, yeast eps15, functions as a multivalent adaptor that coordinates protein-protein interactions essential for endocytosis. J. Cell Biol. *141*, 71–84.

Woodward, M.P., and Roth, T.F. (1978). Coated vesicles: characterization, selective dissociation, and reassembly. Proc. Natl. Acad. Sci. USA *75*, 4394–4398.

Yamabhai, M., Hoffman, N.G., Hardison, N.L., McPherson, P.S., Castagnoli, L., Cesareni, G., and Kay, B.K. (1998). Intersectin, a novel adaptor protein with two eps15 homology and five Src homology domains. J. Biol. Chem. *273*, 31401–31407.

Ye, W., Ali, N., Bembenek, M.E., Shears, S.B., and Lafer, E.M. (1995). Inhibition of clathrin assembly by high affinity binding of specific inositol polyphosphates to the synapse-specific clathrin assembly protein AP-3. J. Biol. Chem. *270*, 1564–1568.

Ye, W., and Lafer, E.M. (1995a). Bacterially expressed F1–20/AP-3 assembles clathrin into cages with a narrow size distribution: implications for the regulation of quantal size during neurotransmission. J. Neurosci. Res. *41*, 15–26.

Ye, W., and Lafer, E.M. (1995b). Clathrin binding and assembly activities of expressed domains of the synapse-specific clathrin assembly protein AP-3. J. Biol. Chem. *270*, 10933–10939.

Zhang, B., Koh, Y.H., Beckstead, R.B., Budnik, V., Ganetzky, B., and Bellen, H.J. (1998). Synaptic vesicle size and number are regulated by a clathrin adaptor protein required for endocytosis. Neuron *21*, 1465–1475.

Zhou, S., Sousa, R., Tannery, N.H., and Lafer, E.M. (1992). Characterization of novel synapse-specific protein. II. cDNA cloning and sequence analysis of the F1-20 protein. J. Neurosci. *12*, 2144–2155.